Title

Flux Creep in a Bi-2212 Rutherford Cable for Particle Accelerator Applications

Journal

IEEE Transactions on Applied Superconductivity, 32(4)

ISSN

1051-8223

Authors

Rochester, Jacob

Myers, Cory

Shen, Tengming

et al.

Publication Date

2022-06-01

DOI

10.1109/tasc.2022.3159267

Flux Creep in a Bi-2212 Rutherford Cable for Particle Accelerator Applications

Jacob Rochester, Cory Myers, Tengming Shen, Milan Majoros, E. W. Collings, and Mike Sumption

***Abstract*— Bi-2212 superconducting cables are being considered for use in the high field magnets needed for the next generation of particle accelerators. Magnetization in these cables and the decay of that magnetization lead to field error and field-error drift, respectively, which need to be compensated. To study this, a segment of the winding pack was extracted from a racetrack coil made from Bi-2212 Rutherford cable. Using a Hall probe measurement technique, we measured the response of the cable's magnetization and its magnetization decay to changes in the applied magnetic field. The effect of adjustments to the cycling of the magnetic field was studied, intended to simulate the preinjection cycles of an accelerator magnet. Three *M* vs. *H* loops were constructed by sweeping the magnetic field applied to the sample from 0 to 2.5 T, then to a preinjection field "x" (where x = 0, 0.25, 0.75 T), and finally up to 1 T. The applied field was then held at 1 T for 1500 s, and the magnetization decay was measured. The decay was found to vary from 8% to 14% after 1500 s, depending on the preinjection field cycle.**

***Index Terms*—Bi:2212, Bi-2212, Magnetization, Creep, Accelerator Magnet**

I. Introduction

The next generation of particle accelerators will require magnets capable of generating very high magnetic fields, 16 T or above [1], [2]. Due to their high critical temperature and high critical magnetic field, high temperature superconductors (HTS), including Bi-2212, are under consideration for use in the windings of such high field magnets. However, many questions pertaining to the behavior of HTS magnets remain unanswered. Among these is quantification of the magnetization and its temporal decay. An understanding of these properties is necessary because magnetization leads to field errors within the bores of the beam steering magnets.

Manuscript receipt and acceptance dates will be inserted here. This work was supported by the United States Department of Energy, Office of Science, Divi-sion of High Energy Physics under Grant DE-SC0011721. Work at LBNL was supported by the Director, Office of Science of the U.S. Department of Energy (DOE) under Contract No. DE-AC02-05CH11231. *(Corresponding author: Ja-cob Rochester.)*

Jacob Rochester, Mike Sumption, Milan Majoros, and E.W. Collings are with the Center for Superconducting and Magnetic Materials, Materials Science and Engineering, The Ohio State University, Columbus, OH 43210 USA (e-mail: rochester.11@osu.edu).

Cory Myers was with CSMM, MSE, OSU. He is now at the Accelerator Technology and Applied Physics division, Lawrence Berkeley National Labora-tory, Berkeley, CA 94720 USA (e-mail: csmyers08@lbl.gov).

Tengming Shen is with the ATAP division, LBNL, Berkeley, CA 94720 USA (e-mail: tshen@lbl.gov).

Accelerator cables and hence magnets exhibit (i) dynamic magnetization, M_{coup}, produced by interstrand coupling currents (ISCCs) [3], [4]; and (ii) static, or hysteretic, magnetization, M_h, resulting from strand-based persistent currents [3], [5], [6]. These magnetizations create bore field distortions expressible in terms of normal and skew harmonics b_n and a_n, respectively. Of these, b_3, the sextupole error component, is usually taken as an index of field quality or error. It depends only on M_h which itself is proportional to $J_c d$, where J_c is the critical current density and d is the diameter of a filament or width/thickness of a tape. Thus, for dipoles wound with multistrand Nb-Ti cable the typical magnetization of magnets are around 10 kA/m, causing a field error on the order of a few units (parts in ten thousand) [7], while those of magnets based on Nb_3Sn are on the order of 200 kA/m and tens of units, respectively [5], [8], [9]. With magnetization values exceeding several hundred kA/m [10], [11], HTS-based magnets could potentially have much larger errors, depending on the design of the conductor and magnet.

While field errors due to static magnetization can be corrected, the time-dependent decay of the magnetization is more difficult to compensate [12]. The magnetization can vary dynamically due to several effects. The interaction of eddy currents with persistent currents, especially eddy currents induced by inhomogeneities in the conductor and in the contact resistance, causes some drift. Inter-strand coupling currents cause exponential decay of the magnetization [3], but this can be mitigated by twisting.

However, HTS materials additionally exhibit flux creep [13]–[16], which causes a decay of magnetization with time that is logarithmic in nature and is measurable for hours. Flux creep arises when the pinning of fluxons is weak relative to the thermal energy of the flux lattice [14]. As such, the HTS materials exhibit high amounts of flux creep at a temperature of 77 K. However, because the pinning is weaker in HTS than in LTS materials, significant flux creep can be seen even at 4.2 K. Therefore, field errors due to flux creep need to be taken into account when designing accelerator magnets, even for use at low temperature.

Magnetization and its decay can be measured readily in a vibrating sample magnetometer; however, the sample space limits these measurements to single wires a few mm long. Moreover, the magnetization behavior of REBCO cables has been shown to differ from that of the tapes from which they are made [11], [17], and that of Bi-2212 cables is strongly dependent on sample length [18]. The necessity to measure cable

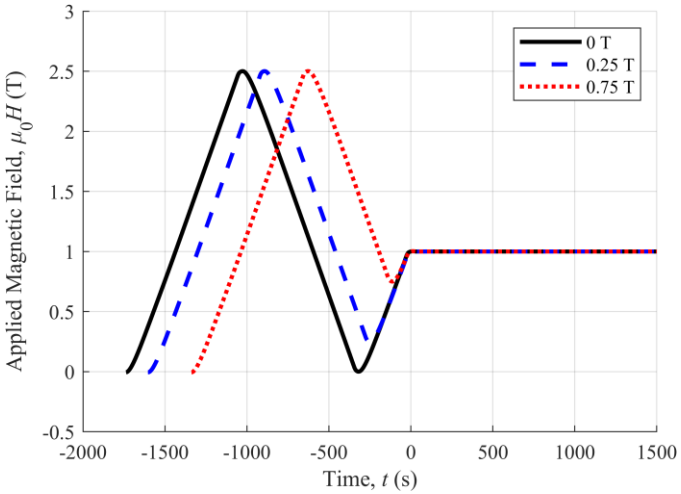

Fig. 1. Applied magnetic field $\mu_0 H$ vs. time t, with $t = 0$ set at the beginning of the dwell at $\mu_0 H = 1$ T. The M vs. H loops reported in [20] were constructed from the $t < 0$ portion, while the decay data reported in this paper were constructed from the $t > 0$ portion.

rather than strand samples, therefore, requires the use of special equipment. Our measurement system, described in [11], allows the measurement of short cable segments up to ~50 mm long in an applied magnetic field of up to 12 T.

Previously, we have reported on the static magnetization of a REBCO tape and cable [11], [17], the dynamic decay of magnetization of a REBCO cable [17], the magnetization and decay in a Bi-2212 strand [18], [19], and the static magnetization of a Bi-2212 cable [20]. In this paper, we report on the dynamic decay of magnetization in a Bi-2212 cable at 4.2 K.

II. Experiment

A. Sample

A series of measurements were performed upon a sample extracted from the epoxy-impregnated racetrack coil RC5, made and tested by LBNL [21], [22]. The sample, 3.9 mm thick x 9.1 mm wide x 30.6 mm long, contained two cable segments. The coil was wound from a 17-strand Bi-2212 Rutherford cable with a cable pitch of 50.8 mm. The cable was made from untwisted Bruker-OST wire, named PMM170123, which contained 18 subelements each with 55 superconducting filaments and was 0.8 mm in diameter before heat treatment. A cross-sectional view of the cable is shown in [20].

B. Measurements

The measurements were performed using the 12 T Hall probe system described in [11], consisting of a liquid-nitrogen-jacketed dewar housed in the bore of a 12 T cryogen-free solenoid. The sample was laid flat against the Hall sensor and inserted into the center of the magnet with the flat side of the cable perpendicular to the applied field. The sample space was then filled with liquid helium.

We determine the magnetization of the sample by subtracting the magnetic field applied externally by the magnet from the measured internal field of the sample according to $B = \mu_0 (H + M)$. For convenience and consistency, we will refer to the applied field as $\mu_0 H$, in units of tesla, the magnetization as M, in units of kA/m, and the magnetic field B inside the sample as the sum of applied field and induced magnetization, also in units of tesla.

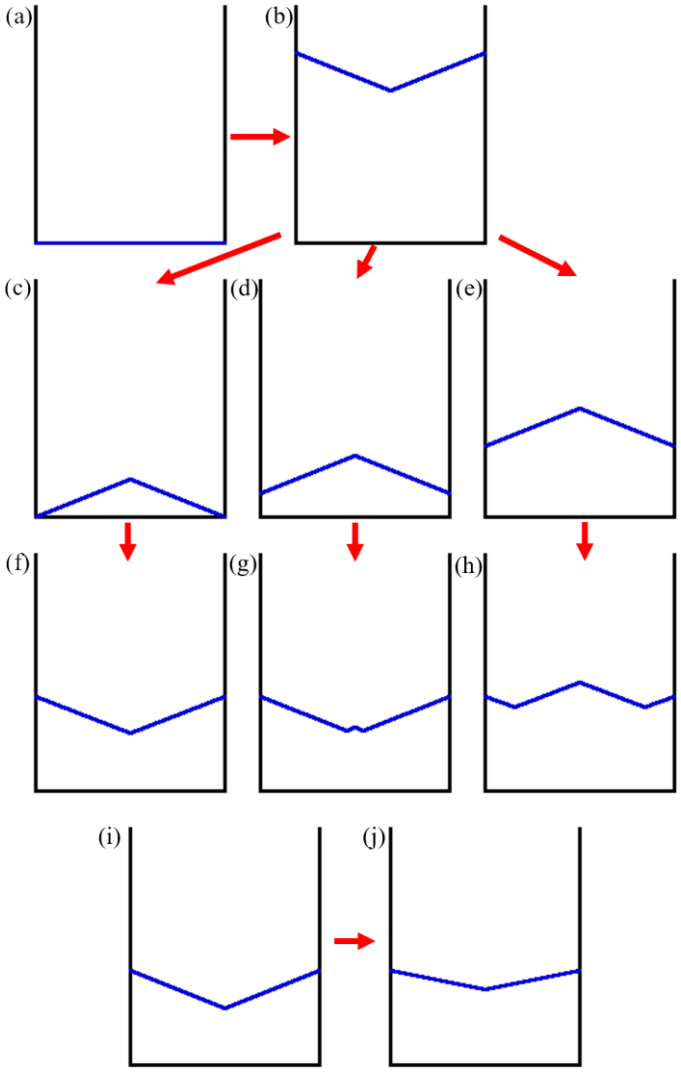

Fig. 2. Simple schematics of Bean magnetization profiles at each step of the field sequence, depicting the internal magnetic field B due to an externally applied magnetic field $\mu_0 H$ and an induced magnetization M, assuming a magnetic field at full penetration of 0.4 T.

The magnetic field was swept in a sequence from 0 T to 2.5 T, to a preinjection hold field "x", to 1 T, and then held for 1500 s. Data acquisition was then ceased and the field was swept to zero. This process was repeated for preinjection hold field values of x = 0, 0.25, and 0.75 T.

The physical origin of the magnetization can be described using a simplified schematic. The magnetic field profile within the sample can be approximated by using the Bean model [23], [24] and representing the sample as a simple infinite slab of superconducting material (Fig. 2).

The applied field initially is 0 T, and the internal field B is 0 T throughout the slab (Fig. 2(a)). The applied field is then swept up to 2.5 T, and the slab is fully penetrated by persistent currents which create a magnetization, M (Fig. 2(b)). Next, the applied field is swept down to the preinjection hold field "x".

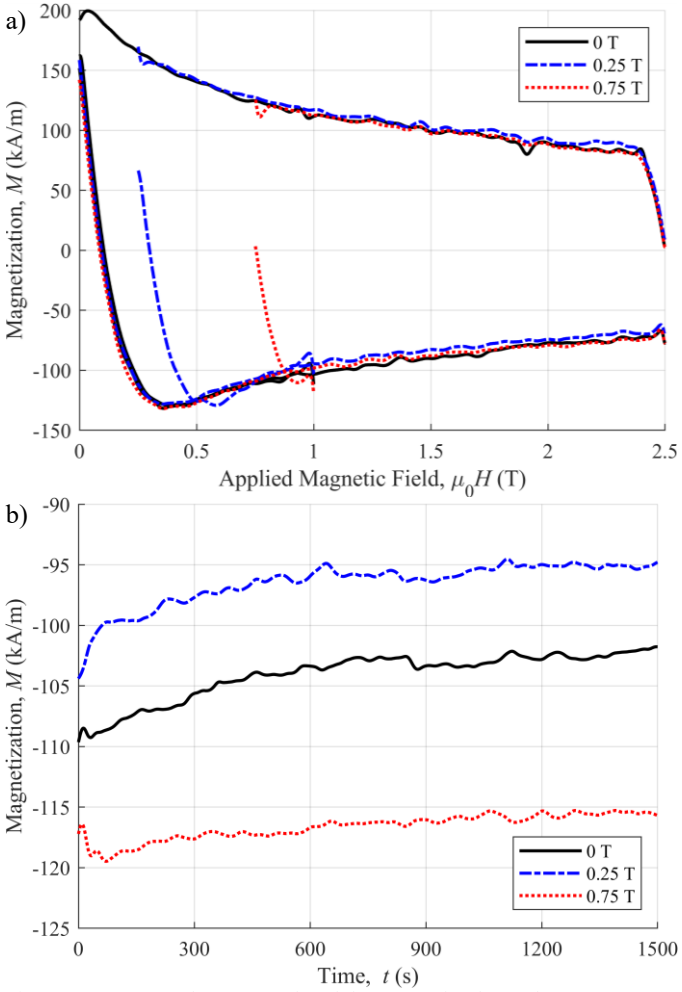

Fig. 3. (a) M vs H loops reproduced from [20] for the cycle 0, 2.5, x, 1 T, where x = 0, 0.25, 0.75 T and (b) the decay of M with time with the applied field held at 1 T immediately following each M vs H loop. Calibrated via Ni replacement and normalized to the volume of wire in the sample. The noise has been reduced using a 51-point gaussian filter, and outliers, perhaps due to mechanical disturbances, which deviated by more than 2σ were removed since they are not relevant to the magnetization phenomenon studied here.

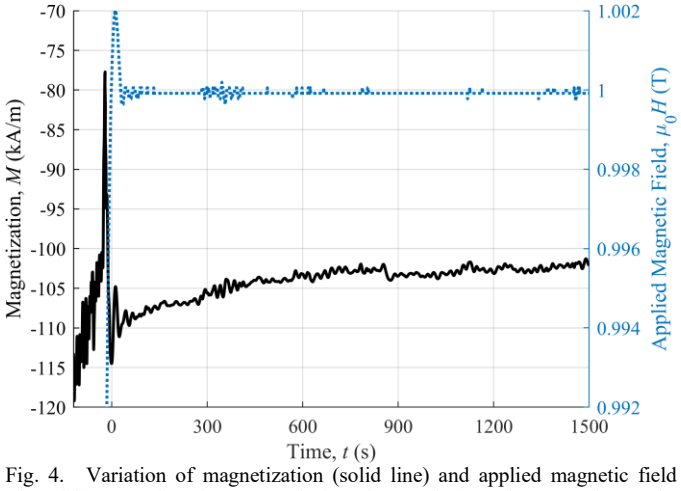

Fig. 4. Variation of magnetization (solid line) and applied magnetic field (dotted line) vs. time from 120 s before the conclusion of an M-H loop. The time t = 0 is set at the first point when the applied field exceeds 1 T at the conclusion of the loop. In this case, an 11-point moving filter was applied to the magnetization to preserve the field and magnetization oscillation around t = 0. All three field sweeps had an analogous overshoot, with slightly differing duration and amplitude.

TABLE I
MEASURED MAGNETIZATION DECAY IN RC5 BI-2212 CABLE

Preinjection Hold Field (T)	Fitted Magnetization at t = 1 s	Fitted Magnetization at t = 1500 s	Decay (%)	r
0	118.2	101.9	13.8	0.0188
0.25	107.8	94.7	12.1	0.0165
0.75	125.0	115.4	7.7	0.0105

For each of the three loops constructed, x = 0, 0.25, and 0.75 T (shown in Fig. 2 (c), (d), and (e), respectively). The applied field is then swept from the preinjection field up to 1 T. The sweep changes the field profile from that seen in Fig. 2(c) to that seen in Fig. 2(f); likewise from (d) to (g) and from (e) to (h). Note that in the cases of x = 0.25 T and x = 0.75 T (Fig. 2 (g) and (h)), the final sweep is not enough to fully reverse the magnetization profile within the slab. Finally, the field is held at 1 T for 1500 s. While the externally applied field does not change during this time, flux creep causes the magnetization to decay, an effect which is logarithmic with respect to time. The relaxation of the magnetization profile due to flux creep for the x = 0 T case is shown schematically in Fig. 2 (i) and (j).

To remove the effect of the surroundings from the data, a background M vs H loop in the absence of a sample, covering 0 to 2.5 to 0 to 1 T was also collected, and magnetization of the background was subtracted from the magnetization measured with the sample present. That this same background loop was subtracted from all three M-H loops is the cause of the discontinuity of the loop at the preinjection step of the x = 0.25 T and x = 0.75 T loops. The signal from the Hall probe at the saturation field of a Ni standard was used to calibrate the data [11], [20]. The data were then normalized to the volume of the wire. The sensor had a sensitivity of 33.72 mV/T; therefore, the conversion factor from Hall voltage to calibrated magnetization was 12.89 μV/(kA/m).

III. RESULTS AND DISCUSSION

In Fig. 3(a) the calibrated M vs H loops previously reported in [20] are reproduced for comparison to the decay response. The magnetization of the Bi-2212 cable at 4.2 K, 1 T was approximately 100 kA/m. By comparison, the Nb-Ti strands used to construct the Large Hadron Collider (LHC) have a magnetization of ~10 kA/m at 2 K, 0.5 T [7], and Nb_3Sn strands developed for the High-Luminosity upgrade to the LHC had a magnetization of 200 kA/m at 4.2 K, 1 T [9]. REBCO magnetization can exceed 900 kA/m in the case of CORC wire [11].

In Fig. 3(b), the variation due to flux creep of magnetization vs. time during the 1 T dwell is shown. Quantification of the decay from start to end of the dwell is complicated by the fact that the magnet power supply did not provide a perfectly linear increasing field to 1 T followed immediately by a perfectly constant field. Instead, the field sweep rate decreased as 1 T was approached, overshot by 2 mT, and then oscillated briefly

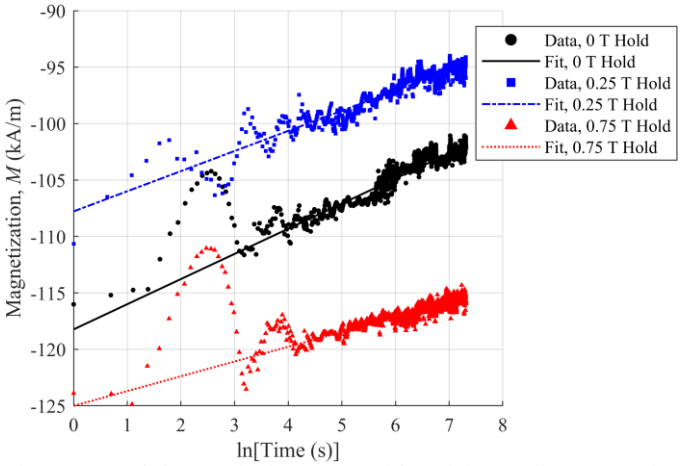

Fig. 5. Recorded magnetization vs natural log of time. A linear regression was used to fit the data after $t = 60$ seconds (by which time the oscillation of applied field and magnetization has mostly stabilized).

about 1 T (see Fig. 4), causing some variation and snapback of the magnetization at the start of the 1 T dwell. As a consequence, the "$t = 0$" at which to measure the initial magnetization must be chosen.

The creep rate can be described by the equation $M = M_0 [1 - r \ln(t)]$ [15], where M_0 is the initial magnetization and r is the creep rate. Thus, magnetization vs time can be linearized by plotting M vs $\ln(t)$ [15]. In Fig. 5, we have plotted the magnetization vs the natural log of time and performed a linear regression on the data beyond 60 s, at which time the applied field is mostly stable. By extrapolating back, we can estimate effective M_0 values at time $t = 1$ s. The magnetization at $t = 1$ s, the magnetization at $t = 1500$ s, the percent change, and the value of r determined by fitting are shown in Table 1. It should be noted that the signal from Hall sensors is known to drift somewhat. A comparison between measurements with and without a sample at constant field found that in the absence of a sample, the Hall probe signal varied by +/- 3 kA/m after 1500 s if calibrated via the same method as our measurements of the sample. This amount of uncertainty is distinct from random noise and might explain the small deviations from the M vs $\ln(t)$ trends in Fig. 5, but it is smaller than the amount of decay observed in the sample.

These creep values, 7.7-13.8% after 1500 s, are much smaller than the 25-45% creep at 1500 s in individual Bi-2212 strands measured by Myers (reported in his dissertation [19, Fig. 27]). It is unclear whether this arises from an intrinsic difference between the two samples, or from a difference between the two measurement systems (a 12 T laboratory magnet in our case vs a Quantum Design PPMS in the case of the individual strands). It is not yet clear whether the lower flux creep in the cable relative to single strands is due to a difference within the samples, the influence of cabling, or the differing measurement approaches.

IV. Conclusion

A segment of Bi-2212 cable was extracted from a racetrack style magnet coil made by LBNL. The magnetization response and decay of the cable at 4.2 K have been measured, simulating multiple choices of accelerator preinjection cycles. In addition, the time-dependent magnetization decay at 1 T after each cycle have been measured. It has previously been shown that flux creep occurs in Bi-2212 at low temperature; this work extends that knowledge to cables relevant for high-energy physics applications. The decay was found to range from 7.7 to 13.8% depending on the preinjection cycle. These values differ from creep values seen in single strands. Future work on this topic should compare direct measurements of cables to measurements of strands extracted from those cables to clarify whether the difference is attributable to a difference within the samples, the influence of cabling, or the differing measurement approaches.

Acknowledgment

Electron microscopy was performed at the Center for Electron Microscopy and Analysis (CEMAS) at The Ohio State University. We thank collaborators within the U.S. Magnet Development Program who contributed to the construction of the RC5 coil, from strand and cable production to coil test.

References

[1] A. Ballarino and L. Bottura, "Targets for R&D on Nb_3Sn Conductor for High Energy Physics," *IEEE Transactions on Applied Superconductivity*, vol. 25, no. 3, pp. 1–6, Jun. 2015, doi: 10.1109/TASC.2015.2390149.

[2] A. Abada *et al.*, "FCC-hh: The Hadron Collider," *Eur. Phys. J. Spec. Top.*, vol. 228, no. 4, pp. 755–1107, Jul. 2019, doi: 10.1140/epjst/e2019-900087-0.

[3] S. Amet *et al.*, "Persistent and coupling current effects in the LHC superconducting dipoles," *IEEE Transactions on Applied Superconductivity*, vol. 13, no. 2, pp. 1239–1242, Jun. 2003, doi: 10.1109/TASC.2003.812643.

[4] A. Jain, "Dynamic Effects in Superconducting Magnets," presented at the US Particle Accelerator School on Superconducting Accelerator Magnets, Santa Barbara, CA, Jun. 23, 2003.

[5] X. Wang *et al.*, "Validation of Finite-Element Models of Persistent-Current Effects in Nb_3Sn Accelerator Magnets," *IEEE Transactions on Applied Superconductivity*, vol. 25, no. 3, pp. 1–6, Jun. 2015, doi: 10.1109/TASC.2014.2385932.

[6] X. Xu, M. Majoros, M. D. Sumption, and E. W. Collings, "Persistent-Current Magnetization of Nb_3Sn Strands: Influence of Applied Field Angle and Transport Current," *IEEE Transactions on Applied Superconductivity*, vol. 25, no. 3, pp. 1–4, Jun. 2015, doi: 10.1109/TASC.2014.2375818.

[7] S. Le Naour *et al.*, "Magnetization measurements on LHC superconducting strands," *IEEE Transactions on Applied Superconductivity*, vol. 9, no. 2, pp. 1763–1766, Jun. 1999, doi: 10.1109/77.784796.

[8] B. Bordini, D. Richter, P. Alknes, A. Ballarino, L. Bottura, and L. Oberli, "Magnetization Measurements of High-J_c Nb_3Sn Strands," *IEEE Transactions on Applied Superconductivity*, vol. 23, no. 3, pp. 7100806–7100806, Jun. 2013, doi: 10.1109/TASC.2013.2240754.

[9] E. W. Collings, M. A. Susner, M. D. Sumption, and D. R. Dietderich, "Extracted Strand Magnetizations of an HQ Type Nb_3Sn Rutherford Cable and Estimation of Transport Corrections at Operating and Injection Fields," *IEEE Transactions on Applied Superconductivity*, vol. 24, no. 3, pp. 1–5, Jun. 2014, doi: 10.1109/TASC.2013.2286860.

[10] M. D. Sumption, E. W. Collings, C. S. Myers, and M. Majoros, "Field Error from Persistent Magnetization and its Decay in Accelerator Magnets Wound with Nb_3Sn, Bi:2212, and YBCO Conductors." unpublished document.

[11] C. S. Myers, M. D. Sumption, and E. W. Collings, "Magnetization and Flux Penetration of YBCO CORC Cable Segments at the Injection Fields of Accelerator Magnets," *IEEE Transactions on Applied Super-*

conductivity, vol. 29, no. 5, pp. 1–5, Aug. 2019, doi: 10.1109/TASC.2019.2896625.

[12] T. Wijnands, L. Bottura, L. Vos, M. Lamont, and A. Burns, "Requirements for real time correction of decay and snapback in the LHC superconducting magnets," CERN-LHC-Project-Note-221, LHC-PROJECT-NOTE-221, Apr. 2000. Accessed: Nov. 05, 2021. [Online]. Available: https://cds.cern.ch/record/691978

[13] P. W. Anderson and Y. B. Kim, "Hard Superconductivity: Theory of the Motion of Abrikosov Flux Lines," *Rev. Mod. Phys.*, vol. 36, no. 1, pp. 39–43, Jan. 1964, doi: 10.1103/RevModPhys.36.39.

[14] Y. Yeshurun and A. P. Malozemoff, "Giant Flux Creep and Irreversibility in an Y-Ba-Cu-O Crystal: An Alternative to the Superconducting-Glass Model," *Phys. Rev. Lett.*, vol. 60, no. 21, pp. 2202–2205, May 1988, doi: 10.1103/PhysRevLett.60.2202.

[15] D. E. Lacey and J. A. Wilson, "Low-field flux-creep measurements on YBCO and BSCCO," *Supercond. Sci. Technol.*, vol. 5, no. 12, pp. 724–731, Dec. 1992, doi: 10.1088/0953-2048/5/12/005.

[16] M. D. Sumption, T. J. Haugan, P. N. Barnes, T. A. Campbell, N. A. Pierce, and C. Varanasi, "Magnetization creep and decay in $YBa_2Cu_3O_{7-x}$ thin films with artificial nanostructure pinning," *Phys. Rev. B*, vol. 77, no. 9, p. 094506, Mar. 2008, doi: 10.1103/PhysRevB.77.094506.

[17] C. S. Myers, M. D. Sumption, and E. W. Collings, "Magnetization and Creep in YBCO Tape and CORC Cables for Particle Accelerators: Value and Modification Via Preinjection Cycle," *IEEE Transactions on Applied Superconductivity*, vol. 29, no. 5, pp. 1–5, Aug. 2019, doi: 10.1109/TASC.2019.2898119.

[18] C. S. Myers, M. A. Susner, H. Miao, Y. Huang, M. D. Sumption, and E. W. Collings, "Reduced Magnetization and Loss in Ag–Mg Sheathed Bi2212 Wires: Systematics With Sample Twist Pitch and Length," *IEEE Transactions on Applied Superconductivity*, vol. 25, no. 3, pp. 1–4, Jun. 2015, doi: 10.1109/TASC.2014.2372614.

[19] C. Myers, "The Influence of Microstructure and Nanostructure on Magnetization and its Temporal Decay in Bi:2212 and YBCO Superconductors at Low Temperatures," The Ohio State University, 2020. Accessed: Nov. 06, 2020. [Online]. Available: https://etd.ohiolink.edu/apexprod/rws_olink/r/1501/10

[20] J. Rochester, C. Myers, M. Sumption, T. Shen, M. Majoros, and E. W. Collings, "The Magnetization of Bi:2212 Rutherford Cables for Particle Accelerator Applications," *IEEE Transactions on Applied Superconductivity*, vol. 31, no. 5, Art. no. 6400305, Aug. 2021, doi: 10.1109/TASC.2021.3059985.

[21] T. Shen *et al.*, "Stable, predictable and training-free operation of superconducting Bi-2212 Rutherford cable racetrack coils at the wire current density of 1000 A/mm^2," *Scientific Reports*, vol. 9, no. 1, p. 10170, Jul. 2019, doi: 10.1038/s41598-019-46629-3.

[22] T. Shen and L. Garcia Fajardo, "Superconducting Accelerator Magnets Based on High-Temperature Superconducting Bi-2212 Round Wires," *Instruments*, vol. 4, no. 2, Art. no. 2, Jun. 2020, doi: 10.3390/instruments4020017.

[23] C. P. Bean, "Magnetization of Hard Superconductors," *Phys. Rev. Lett.*, vol. 8, no. 6, pp. 250–253, Mar. 1962, doi: 10.1103/PhysRevLett.8.250.

[24] C. P. Bean, "Magnetization of High-Field Superconductors," *Rev. Mod. Phys.*, vol. 36, no. 1, pp. 31–39, Jan. 1964, doi: 10.1103/RevModPhys.36.31.